FREIA Report 2012/04
November 2012

UPPSALA UNIVERSITET

DEPARTMENT OF PHYSICS AND ASTRONOMY
UPPSALA UNIVERSITY

Proposal for Design and Test of a 352 MHz Spoke RF Source

ESS TDR Contribution

V.A. Goryashko (ed.), D. Dancila, T. Ekelöf, K. Gajewski, L. Hermansson, N. Johansson, T. Lofnes, M. Noor, R. Ruber, A. Rydberg, R. Santiago-Kern, R. Wedberg, R.A. Yogi, V. Ziemann

Uppsala University, Uppsala, Sweden

Department of
Physics and Astronomy
Uppsala University
P.O. Box 516
SE – 751 20 Uppsala
Sweden

Papers in the FREIA Report Series are published on internet in PDF- formats.
Download from http://uu.diva-portal.org

Uppsala University
FREIA Group

29th November 2012

vitaliy.goryashko@physics.uu.se

Proposal for Design and Test of a 352 MHz Spoke RF Source

V.A. Goryashko (ed.), D. Dancila, T. Ekelöf, K. Gajewski, L. Hermansson, N. Johansson, T. Lofnes, M. Noor, R. Ruber, A. Rydberg, R. Santiago-Kern, R. Wedberg, R.A. Yogi, V. Ziemann
FREIA Group, Uppsala University

Contents

1 Introduction **2**

2 Requirements **3**

3 High-power RF amplifier **5**
3.1 Tetrode amplifier 5
3.2 Schematic of the high-power RF system 6
3.3 Details regarding TH595 operation 8
3.4 Preamplifier for high-power tetrode 10
3.5 Summary 11

4 RF system **11**
4.1 RF distribution 11
4.2 Diagnostic and RF hardware 14
4.3 Control system 14

5 Tetrode power supply **15**
5.1 Anode power supply 16
5.2 Screen grid power supplies 18
5.3 Control grid power supplies 19
5.4 Filament power supplies: 20
5.5 Possible technical risks 20
5.6 The start-up sequence of the power supplies 20

6 High-power RF test at the FREIA Facility **21**
6.1 Power supply test 21
6.2 Testing of the high-power amplifier and components 22
6.3 High-power test of the ESS spoke cavity 23
6.3.1 Cavity test stand 24
6.3.2 Measurement of the accelerating gradient 25
6.3.3 Study of the Lorentz detuning 25
6.3.4 Study of the piezoelectric tuner action 26
6.3.5 Conditioning the cavity coupler 26
6.4 Summary 26

References **27**

1 Introduction

Uppsala University is erecting the FREIA facility in order to participate in the development of the radio-frequency (RF) system for the European Spallation Source (ESS). FREIA was initiated under high time pressure at the request of the ESS and in order to be ready for testing a first spoke cavity in 2014 and the first prototype spoke cryomodule in 2015. FREIA will also prototype the high power RF source for the ESS poke LINAC. A suitable high-power source for testing has to be built and need to be procured in a timely fashion. The key parameters of the power generator are to provide up to 300 kW for duration of almost 4 ms at a repetition rate of 14 Hz.

A survey of suitable sources has been published earlier [1], [2] and compared tetrode, lOT, solid-state and klystron based options. A tetrode based option is considered the best choice with todays available technology and is therefore considered preferable for the FREIA test stand to get started in a timely fashion. The ESS Accelerator Internal Review (AIR) committee expressed concern about the tetrode based option as tetrode amplifiers do not exist at the ESS specification and the AIR recommended to re-evaluate the solid-state amplifier option for the final ESS spoke power source. But as off-shelf solid state amplifiers do not exist at the ESS specifications, the ESS accelerator technical advisory committee (aTAC) agreed that a tetrode based amplifier is the best solution for the first amplifier chain at FREIA.

This report describes the design of a tetrode based RF power source for the FREIA test stand which must be available for high-power tests of one spoke cavity by 2014. The spoke cavity components and physical effects that need special care and comprehensive testing are discussed along with cavity testing techniques and setup. Upon completion of the high-power spoke cavity tests, Uppsala University will perform tests of a spoke-cryomodule containing two cavities. These tests will require a second amplifier chain. In parallel to the development of the tetrode based system we are investigating the suitability of solid-state based amplifiers for the second amplifier chain. If these tests are successful we intend to replace the tetrode in the first drive chain by a solid-state amplifier at a later stage.

2 Requirements

The ESS LINAC [3] has twenty-eight superconducting spoke cavities operating at a frequency of 352 MHz that accelerate the proton beam with an intensity of up to 50 mA from 80 MeV to 200 MeV. According to the baseline RF design, there is a single RF amplifier per (spoke) cavity. The required power transferred to the beam ranges from 162 to 239 kW [4]. Including 5 % for losses and a 15 % overhead for the LLRF system we find that power levels of up to 300 kW are required. The time structure of the beam is that individual bunches spaced by the RF period of 2.84 ns form a pulse train with a length of 2.86 ms. The pulse trains are generated with a repetition rate of 14 Hz.

These requirements directly determined the specifications for the RF power amplifiers. They need to provide 300 kW with a repetition rate of 14 Hz for a duration at least of 3.5 ms which is slightly longer than the beam pulse to permit filling the cavity to an appropriate level. Moreover, the center frequency of the amplifier needs to agree with the bunch frequency of $f_0 = 352$ MHz. The loaded Q of the cavity (Q_L) is of the order of 150 000 [5], which sets the requirement for the 3 dB bandwidth of the amplifier. We specify that the power amplifier must have a 3 dB bandwidth of at least 100 times the bandwidth of the cavity $f_0/Q = 2.35$ kHz for appropriate stabilization of the cavity voltage and phase. We thus arrive at a bandwidth requirement for the amplifier of 250 kHz. The natural cavity filling time, $t_F = 2Q_L/\omega = 135\mu$s, dictates the temporal performance of the amplifier. Apart from meeting the base requirements we request that the system has to operate with high efficiency in order to be economical. The RF system requirements are summarized in Table 1.

One of the main purposes of the high-power test, apart from testing the cavity itself, is the implementation of a reliable and automatized adaptive feed-forward compensation system. To this end the cavity tuner and corresponding hardware have to be tested under realistic conditions. Specifically, the shape of the cavity voltage pulse has to be the same as expected to be in the cavity operating in a LINAC. This implies the cavity voltage has to reach

Table 1: *RF system requirements.*

Frequency	352.21	MHz
Repetition rate	14	Hz
Beam pulse length	2.86	ms
Maximal power to beam	240	kW
Maximal power to cavity	270	kW
Power overhead for control	15	%
Power overhead for losses (in distribution)	5	%
Amplifier output power	300	kW
Bandwidth at 3 dB	>250	kHz
RF pulse length [1]	3.5	ms

[1]The RF pulse length has to exceed at least the sum of the beam pulse length and the time required to pre-fill the cavity. The latter is dictated by the optimal beam injection time equaling 80μs. Recall that the optimal beam injection time, t_{inj}, is related to the natural cavity filling time, $t_F = 2Q_L/\omega$, by $t_{inj} = t_F \log(I_g/I_b)$ [6], where I_g and I_b are the generator and beam currents, respectively.

nominal accelerating voltage of 5.1 MV by the moment of the expected beam injection time that is around 80 μs. Then, flat-top operation of the cavity should be kept on. To obtain such a voltage pulse shape without beam, pulsed RF power with a special step-wise shape is fed to the cavity [7], [8], [9]. Initially, a pre-pulse with a power of around the desired maximal power to beam is applied to quickly charge the cavity by the moment of the expected beam injection time, then the power is dramatically reduced to one-forth of the maximal beam power [10]. The targeting cavity voltage and the incident power required to feed the cavity as a function of time for the ESS spoke cavity are shown in Fig. 1. Although the shift of the cavity frequency caused by the Lorentz force is moderate due to the high stiffness of the cavity, see the left plot in Fig. 2, the cavity phase change is substantial as it is shown in the same Fig. 2 on the right. These simulations were performed for a static Lorentz detuning

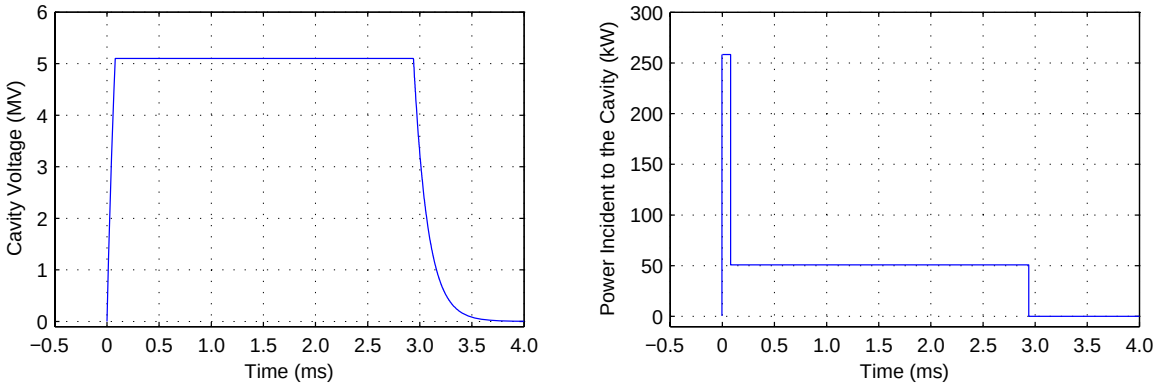

Figure 1: The cavity voltage (on the left) and the power incident from the coupler to the cavity (on the right) as a function of time. The beam injection time in the accelerator is around 80 μs so that the cavity is charged to the nominal value of 5.1 MV during this time and then flat-top operation is keeping up. Since there is no beam injection at 80 μs the power is dropped in order to not overcharge the cavity. The Lorentz force detuning is ignored in the simulation of the cavity voltage.

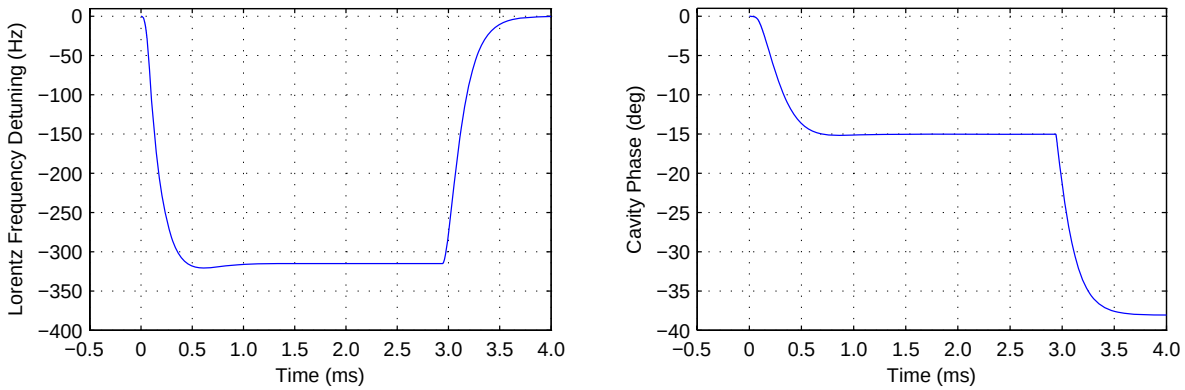

Figure 2: The Lorentz force detuning and the cavity phase vs. time calculated for the voltage distribution shown in Fig. 1.

coefficient of -5.3 Hz/(MV/m)^2 assuming free cavity ends [11]. From Fig. 1 it is clear that to perform cavity testing the amplifier should be able to reach high-power within several tens of microseconds and also be able to quickly change the power level without phase jump to model the beam effect during the high-power test of the spoke cavity.

The purpose of the FREIA facility is to construct a prototype of RF power generation system able to meet the requirements specified above, test the performance of its components as well as the RF system, first coupled to a single prototype spoke cavity in a cryostat, followed later by system tests of the ESS spoke cryomodules containing two spoke cavities. The FREIA RF system schematically shown in Fig. 3 will consist of a signal generator, power amplifier, RF distribution system, LLRF control system, diagnostic hardware and the cavity.

In the following sections we describe first the power amplifier and how we arrived at the choice of layout as well as components, mainly the selected tetrode tube. We then discuss the required preamplifier and the RF distribution system, followed by a discussion of the diagnostics. We then address the control system and choice of power supplies and conclude by discussing the test program that we envision for the coming years: first tests of the power supplies, then the tetrode amplifier into a dummy load and finally tests with a single spoke cavity and later with the cryomodule.

But we start with the discussion of the high power amplifier.

3 High-power RF amplifier

3.1 Tetrode amplifier

The central component of the high power amplifier is the tetrode and a survey of the field has resulted in three tetrodes, all manufactured by Thales, that are potentially suitable candidates.

The TH781 [12] is normally used at lower frequencies up to 200 MHz but it can also produce 300 kW pulses at 352 MHz albeit at a reduced gain of 13 dB and with an efficiency

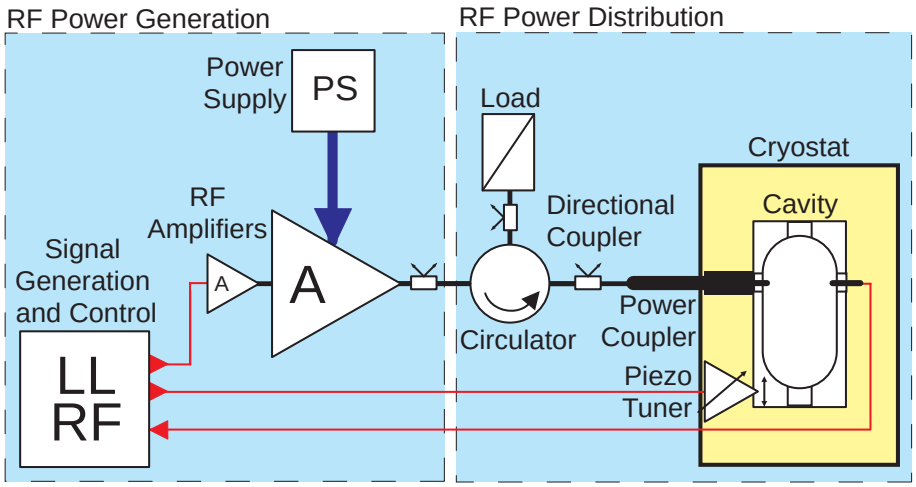

Figure 3: Conceptual layout of the FREIA RF system.

of only 55 %.

The TH391 [13] offers an improved gain of 15 dB and an efficiency exceeding 65 %. It is, however, air cooled and only allows a rather limited anode dissipation of 12 kW CW. Moreover, air cooling results in a larger system size.

The TH595 [14] can only operate at power levels of up to 200 kW in a pulsed regime (tested with a duty cycle of 2.5%) such that we need to combine two tubes to achieve 300 kW. But the gain exceeds 15 dB and an efficiency of 65 % is sufficiently high. Another advantage is that it is water-cooled and therefore can sustain a higher anode dissipation of up to 40 kW CW. Finally, there exists the design of an output cavity, which caused us to select the TH595 for the first amplifier in FREIA. Recently, Thales has tested the TH595 tetrode with the TH18595 cavity at the ESS specifications on a matched load [15]. The gain, efficiency and peak power around 15 dB, 65% and 200 kW, respectively, were achieved. The amplifier was also tested at long pulses of 5 ms with a peak power up to 210 kW. The summary on a comparison of the tetrodes can be found in Table 2.

3.2 Schematic of the high-power RF system

The basic layout of the FREIA amplifier design is shown in Fig 4. The first hybrid coupler H1 just downstream the signal generator SG divides the signal with a power of the order of a few mW into two equal-amplitude components with a 90^o phase difference, which drive the two pre-amplifiers A1 and A2. The 10 kW power outputs of the pre-amplifiers are amplified in the high-power tetrode amplifiers PA1 and PA2 up to 150 kW. Each tetrode amplifier output is protected by means of circulator from reflected power. Outputs of both tetrodes also have a relative phase shift of 90 degrees. The second hybrid coupler H2 downstream PA1 and PA2 recombines the amplifier outputs to produce 300 kW power. Any phase shift and amplitude errors can be corrected with the help of an attenuator and phase shifter present after the signal generator. The tetrode amplifiers are the key elements of the amplifier scheme since they have to amplify the RF signal with a moderate power level produced by the pre-amplifiers up to 150 kW output power in each tetrode The nominal operating requirements on the tetrode amplifier are listed in Table 3.

To use standard RF components for the RF distribution system the input of the tetrode should be a 50 Ohm coaxial connection. As the input power is of the order of 10 kW, 7/8 inch 50 Ω line can be used as an input to the tetrode. The output power is 150 kW so that a

Table 2: *Typical performance of tetrode tubes, f_0 = 352.21 MHz.*

Specification	TH391	TH595	TH781	
Pulse width	250	100/CW	CW	μs
Duty cycle	2.5	5.0/100	100	%
Max. power at f_0	200	200/30	350	kW
Efficiency	>60	>65	50–55	%
Gain	15	15	11	dB
Output cavity f_0	TH18230B	TH18595A	to be developed	
Cooling	air	water	water	

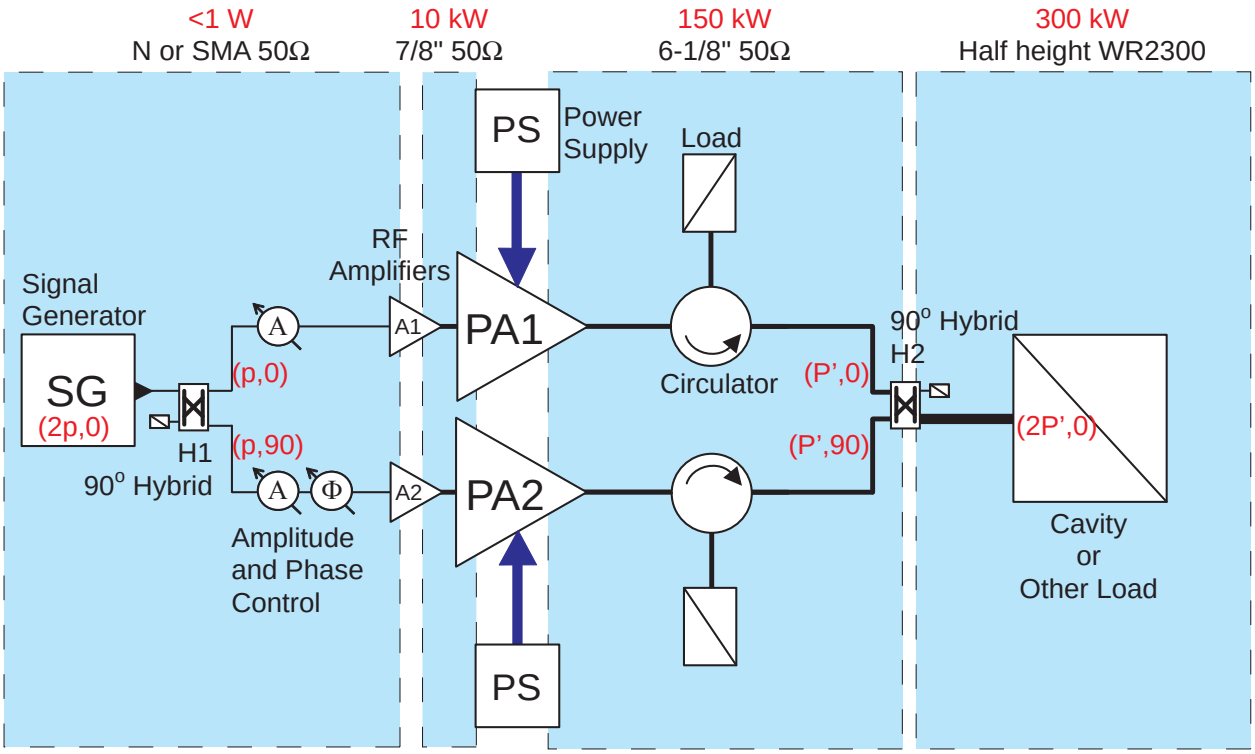

Figure 4: Schematic of the FREIA amplifier and RF distribution layout for the first chain at the Uppsala test stand. SG: signal generator, Φ: phase shifter, A: attenuator, A1, A2: preamplifiers, PA1 and PA2: high-power amplifiers. The type of an RF distribution line and the nominal transmitted power are specified in the top part of the schematic.

Table 3: *Tetrode performance requirements.*

Frequency	352.21	MHz
Bandwidth at 3 dB	>250	kHz
Repetition rate	14	Hz
RF pulse length	> 3.5	ms
Gain	> 15	dB
Maximal power	> 150	kW
Lifetime	> 20000	h
Type of input connection	coaxial line	
Size of input connection	7/8	inch
Input impedance	50	Ω
Input power	< 10	kW
Type of output connection	coaxial line	
Size of output connection	6-1/8	inch
Output impedance	50	Ω

transmission line able to handle such power is needed and we propose to use the 6-1/8 inch 50 Ω coaxial line as an output line. The outputs of the two tetrodes are combined to produce 300 kW using a hybrid coupler. To transport 300 kW we propose to use half height WR2300 waveguide that is more compact than full height WR2300 waveguide but can handle 300 kW. As a result, the hybrid coupler will make use of a half height WR2300 waveguide as well. During the transient regime with a duration of the order of 100 μs a substantial part of the forward power is reflected by the spoke cavity. The reflected energy, defined as an integral of the power over time, may be estimated as 30 J. In the tests without beam the reflected power during the 2.86 ms cavity flat-top operation (duration of the flat-top operation has to correspond to the beam duration) is expected to be around 50 kW such that the reflected energy will be 150 J. The total reflected energy is up to 200 J but the tetrode can sustain only around 20 J per pulse, therefore the output of the tetrode must be protected by a circulator.

3.3 Details regarding TH595 operation

The tetrode TH595 is a ceramic-metal tetrode with a coaxial structure and forced water cooling. The maximal ratings of the tube are presented in Table 4. Apart from suitable RF characteristics this tube being compact and light allows for simple installation and maintenance. Currently, tetrodes TH595 are used for various applications, for example, in the Institute for Plasma Research, IBA-Group and CERN-CH [16].

It is well known [17] that gain of the tetrode reduces with aging. While calculating the power needed from the pre-driver, this fact was taken into consideration in order to have a margin in terms of driving power, so a conservative gain of 13 dB is assumed and consequently the required output power of the pre-driver is 10 kW.

Table 4: *Maximal ratings of TH595.*

Frequency	352	MHz
Maximal power	200	kW
Anode Voltage	18	kV
Anode direct current	9	A
Maximal anode dissipation	40	kW
Peak cathode current	45	A
Screen grid voltage	1.3	kV
Control grid voltage	-400	V
Screen grid dissipation	150	W
Maximal operating frequency	450	MHz
Anode cooling	water	
Screen grid cooling	air	
Cathode	thoriated tungsten	
Length	228	mm
Diametre	114	mm
Weight	7.2	kg

A right choice of the class of tube operation affects not only the tube's efficiency and gain but also the lifetime [18]. In class C operation the efficiency is the highest but nonlinearity and higher harmonic content in the output wavefront are also the highest. The other penalty to be paid for this increase in efficiency is a reduction in gain because the tube must be driven harder. We propose to operate the tetrode TH 595 in class B instead, thus achieving lower harmonic distortion than class C but higher efficiency (around 65%) than in class A. Operating in class B implies that a quiescent current is flowing in the time between beam pulses such that power will be dissipated before and after the RF pulse [17]. To avoid this either the cathode grid or screen grid power supply will be modulated, *i.e.* it should be made more negative before and after the RF pulse to get nearly zero quiescent current.

The proposed amplifier will operate as a grounded grid tube. One tetrode requires four power supplies, but for the two tetrodes in the overall amplifier only seven power supplies are required by combining the anode power supplies. The requirements and architecture of the power supply are discussed in detail in section 5.

The tube has a water cooled anode and an air cooled filament. The calculated requirements on cooling are given in Table 5. Appropriate cooling is important for a reliable tube operation, thus the following parameters have to be monitored during the operation:

- inlet water pressure;
- water flow;
- outlet water temperature;
- water resistivity;
- air inlet pressure;
- air flow and/or outlet air temperature.

The amplifier should also include protections to react to the forward and reflected powers, thermal overload and failure of any component.

The technology of the tetrode has already been well proven in accelerator applications [19] and this tube benefits from the robustness and reliability in operation [20]. Although the maximal tetrode lifetime is short as compared to the klystron and is around 20 000 hours, the analysis of the gain decrease allows to control the remaining lifetime and plan the tube

Table 5*: Cooling requirements for TH 595.*

Anode Cooling		
Water flow rate	> 20	lpm
Resistivity at 20^oC	> 500	kΩ-cm
Filament cooling		
Air flow at 30 mbar	> 2	m^3/min
Air flow at 10 mbar	> 4	m^3/min

replacement. In fact, the tetrode TH595 uses the so-called thoriated-tungsten cathode, which is created in a high-temperature gaseous atmosphere to produce a layer of di-tungsten carbide on the surface of the cathode [14], [21]. Thorium is added to tungsten to decrease the thermo-emission work function, thus resulting in an increase in emission current. So, cathode characteristics are dictated by the surface properties, and a thoriated-tungsten cathode demonstrates decrease in emission when most of the carbon has evaporated, depleting the internal double electrical layer [22]. The process of cathode deterioration is slow and an analysis of the gain decrease allows to control the re-maining lifetime and plan the tube replacement. For example, operational experience at CERN [2] also indicates that a tetrode does not fail at an unpredictable moment but instead it demonstrates features of deterioration, appearing as a decrease in gain that allows to plan maintenance and replacement before it becomes unreliable [19]. Each tetrode in the FREIA amplifier will be operated only at around 70% of the maximal output power specified by the manufacturer such that its mean lifetime approaches the maximal lifetime. Therefore, we may expect that each tetrode will serve at least two years before it requires replacement [3].

3.4 Preamplifier for high-power tetrode

The gain of the tetrode is low (the worst case of 13 dB gain is considered) and an input power of 10 kW is needed to drive the tube and reach the nominal power of 150 kW at the tetrode's output. At the same time, output power of a signal generator is typically in the mW range so that an intermediate amplification stage is needed. The main requirement on the pre-driver amplifier is a very high gain that has to be more than 70 dB. Along with a high gain the pre-driver amplifier must not limit performance of the whole amplifier such that a high efficiency, sufficient 3 dB bandwidth and good reliability and lifetime are important as well. The requirements on the pre-driver amplifier are summarized in Table 6. Comparison of available RF sources strongly indicates that a solid-state amplifier (SSA) is one of the most rational and reliable solutions.

In fact, the SSA concept is based on a highly modular design: built-in redundancy improves reliability. The mean time between failures of high-power SSAs is more than 1 year [23]. For example, solid state amplifiers with the power levels up to 35 kW and 190 kW at 352 MHz are operated on the SOLEIL storage ring. From their commissioning in 2004 and 2006, respectively, these systems were proven to be reliable and have not yet caused any beam time loss [24]. Due to a high proven reliability the SSA is chosen for the MYRRHA project, in which reliability is the most crucial issue as it should be at the same level as the reliability of a nuclear reactor [25]. We propose to use SSA as a pre-driver amplifier for the tetrode amplifier.

[2] 200 MHz RF SPS system has one station with 20 tetrodes, water cooled, and another one with 86 tetrodes, air cooled.

[3] The ESS expected annual operating time is 5200 h (see CDR/TDR table 1.2), so the expected LINAC RF operation time is somewhere between 5200 h and 8700 h of a full year whereas the tetrode lifetime is around 20 000 h.

Table 6: *Requirements on the pre-driver performance*

Central frequency	352.21	MHz
Bandwidth	1	MHz
Repetition rate	14	Hz
RF pulse length	> 3.5	ms
Nominal power	10	kW
Efficiency	>65	%
Gain	70	dB
Lifetime	> 100000	h
RF rise/fall time	1	μs
Input/output impedance	50	Ω
Connections	SMA or N-type	
Cooling	water preferred	
VSWR	< 1.2	

3.5 Summary

Tetrodes have many decades of excellent operational records and do not fail unpredictable but deteriorate slowly so replacement can be scheduled within regular maintenance periods. Solid-state amplifiers have extremely high reliability due to its built-in redundancy, low trip rate and long lifetime. Therefore, the tetrode amplifier with a solid-state pre-driver is a highly reliable system.

4 RF system

4.1 RF distribution

Transfer of an RF signal from the signal generator through the amplifying stages to the spoke cavity is performed by the RF distribution line discussed in Sec. 3.2. The requirements include the amount of power that the system is capable of handling, protection of the amplifier from reflected power as well as low level RF diagnostic and control. The insertion loss has to be below 5%. Minimal length and simplicity of the overall system are of significant importance as well. As shown in Fig 4, there are four power levels, so there should be more than one type of RF distribution line. The characteristics of proposed RF lines are summarized in Table 7.

The spoke cavity will be located in a cryostat in a bunker to provide protection against X-ray and gamma radiation as well as RF field in case of leakage. Using the actual 3D model of the bunker a corresponding physical 3D layout of the RF distribution system was created as shown in Figs. 5,6.

As we discussed above the spoke cavity may reflect energy up to 200 J but the tetrode can sustain only 20 J per pulse so that a circulator has to be used. The standard isolation of a commercial circulator is better than 20 dB. This means that less than 1 J of the reflected energy will be seen by each tetrode and thus standard circulator isolation is sufficient.

The circulator can be used either immediately after the tetrode or after combining the two outputs, *i.e.* downstream the hybrid coupler. The size of a circulator using 6-1/8 inch coaxial line is only 0.6m x 0.6m x 0.5m, whereas the size of the circulator in half height WR2300 waveguide is 2.5m x 2.5m x 0.5m. Hence, a circulator in 6-1/8 inch coaxial line used immediately after the tetrode amplifier is a more reasonable choice. As the power level is low, the circulator does not need a temperature compensation loop, but needs needs an

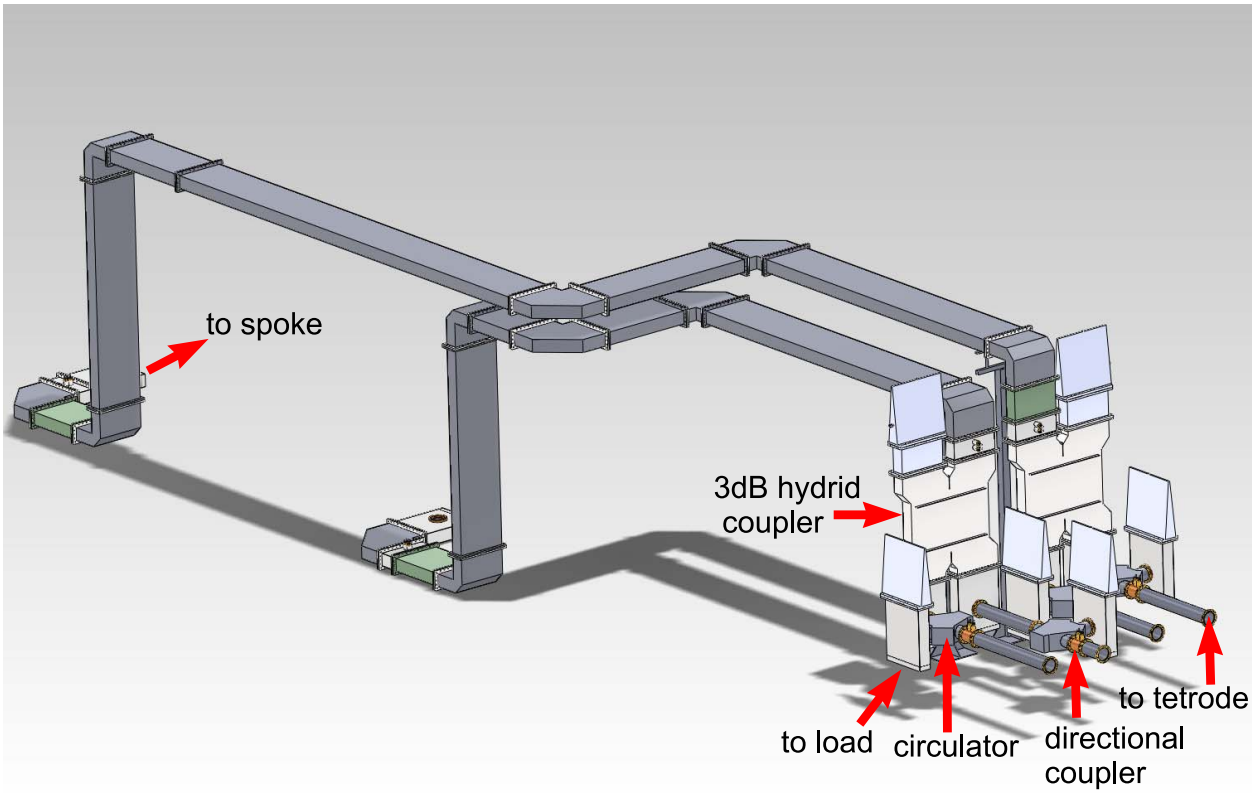

Figure 5: Layout of the RF distribution system from the circulators to the spoke cavity couplers.

Table 7: *Parameters of the RF distribution line. Connection sectors are denoted by Roman numerals I: signal generator to pre-driver, II: pre-driver to tetrode, III: tetrode to hybrid coupler, IV: hybrid coupler to spoke coupler.*

	I	II	III	IV
Nominal power	mW	10 kW	150 kW	300 kW
Type of connection	cable	coaxial line	coaxial line	WR2300
Size	N/SMA	7/8 inch	6-1/8 inch	half height
Maximal power	W	50 kW	1 MW	10 MW
Bandwidth (all lines)			>2 MHz	
Power loss (all lines)			< 0.05 dB	

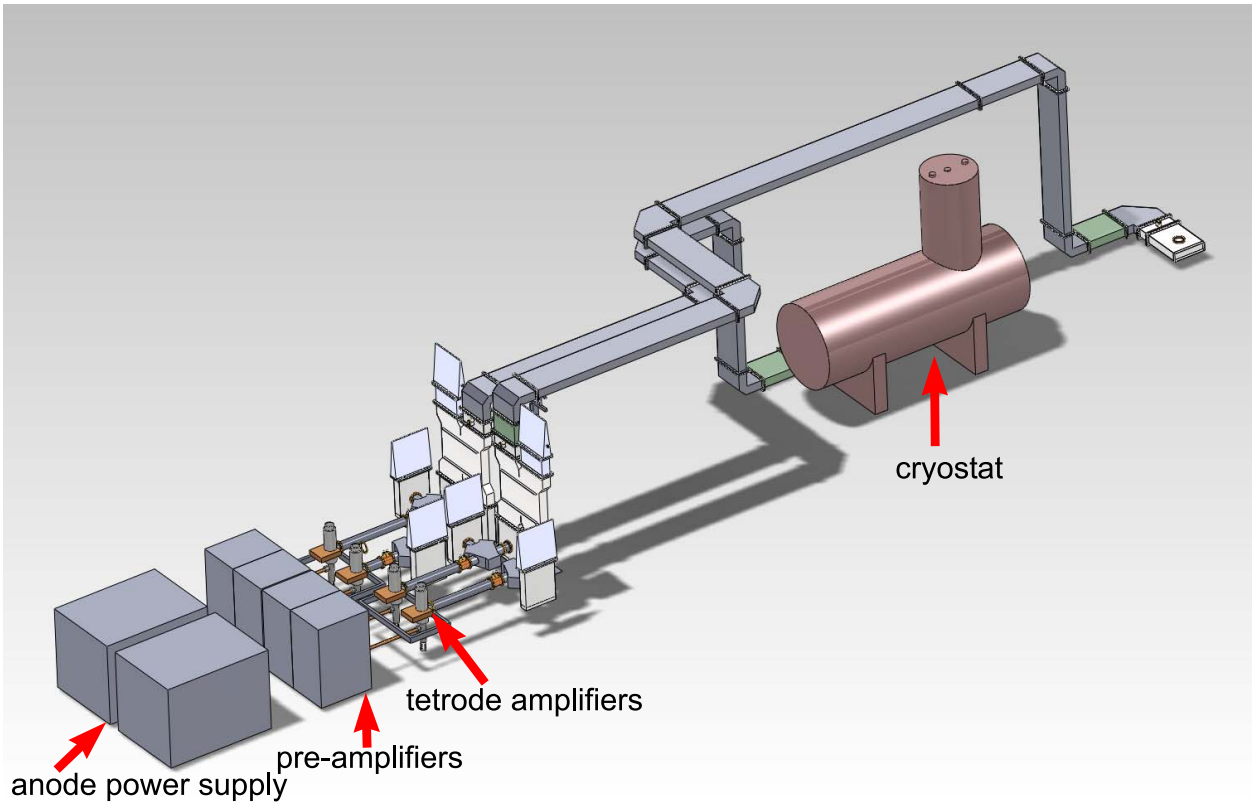

Figure 6: Complete layout of the RF distribution system

electromagnet compensating for changes in the return loss of the circulator.

A dummy load is connected to the third port of the circulator so that under mismatch conditions the power reflected from the cavity is absorbed in the dummy load. The dummy load can either be water or ferrite load. A water load needs an RF window separating coolant from the waveguide. The coolant used is ethylene-glycol water mixture. There are chances that the window may develop cracks leading to water leakage inside the RF system. Therefore, a ferrite load is preferred over a water load. Unfortunately, due to construction difficulties ferrite loads are available only in waveguide geometry: ferrite load with half height WR2300 can be used along with a 6-1/8 inch coaxial to waveguide adapter. Each tetrode chain will then need one of such arrangement.

To satisfy the requirement on the RF distribution system loss the return and insertion loss of all the components in the RF distribution system components needs to be better than 30 dB and 0.05 dB, respectively. In order not to limit bandwidth of the power source, the bandwidth of all the components in the RF distribution system needs to be greater than the pre-driver bandwidth and is set to 2 MHz.

Each part of the RF distribution system (7/8 inch and 6-1/8 inch) needs to have dual directional couplers to monitor forward and reflected power. Since FREIA is the test facility directional couplers should be installed after the pre-driver, tetrode amplifier, circulator, hybrid coupler and upstream the spoke cavity. Diagnostic hardware works with a power level of mW so that directional couplers will be complemented with additional attenuators after the coupler output in order to outcouple a part of the RF power that can be directly

used for data processing.

The hybrid coupler H2 at the end of the amplifier chain will combine the power to 300 kW and has to sustain the reflected power. At the Fermi Laboratory [27] the 325 MHz hybrid coupler based on WR2300 waveguide geometry was tested under full reflection condition up to 170 kW CW and showed good performance. According to the manufactures specifications, such a coupler can handle more than 1 MW so that the hybrid coupler based on WR2300 geometry is proposed for the FREIA amplifier. As the maximum power carrying capability of the half height WR2300 is more than 10 MW, it is selected for the RF distribution at 300 kW power. Note that the 6-1/8 inch coaxial line can also be used for RF distribution, but the installation and cooling becomes difficult as it contains inner conductor, outer conductor, inner conductor joints and either teflon or ceramic rods to support inner conductor inside the outer conductor. Hence the length of 6-1/8 inch coaxial line section is kept to a minimum and used only to transmit RF power from the tetrode output to the hybrid coupler H2 input.

The distribution system also needs flexible waveguides to take care of mechanical alignment. Specifically, each RF distribution system may need one or two flexible waveguides to take care of mechanical assembly, thus having one or two per tetrode chain. Bends for bending the coaxial line are needed as well.

4.2 Diagnostic and RF hardware

We anticipate to use directional couplers to monitor the forward and reflected power, both at the amplifiers and at the cavity. The signals coming from the directional couplers and from the cavity probe are going to be directly down converted to baseband by using fast ADCs sampling at 150 MSa/s. These ADCs do have an input bandwidth greater than 400 MHz. This makes it possible to use the so-called under-sampling technique, or bandpass sampling, if the signals are first filtered with a bandpass filter. The bandpass filter needs to have a center frequency of 350 MHz and a bandwidth of less than 75 MHz. With this technique there is no need for any mixers to down-convert the signals. I and Q demodulation of the signals are made in software with the help of digital signal processors. Further reduction of the bandwidth will also be made with software. The low level drive signal to the cavity will be furnished by a direct digital synthesizer (DDS).

4.3 Control system

The control system for FREIA will be based on EPICS (Experimental Physics and Industry Control System), the same system that is planned to be used in ESS. EPICS is a distributed system consisting of a number of the so-called Input/Output Controllers (IOC) usually equipped with the hardware interfaces to the controlled process, server computers running services like archiving, logging, alarm and the desktop computers used as operators consoles. All these units are interconnected using the Ethernet network.

The control system will consist of at least one IOC (based on the same hardware and software as that developed at ESS, called by them ControlBox), an operator console (one or more) and a server for archiving, logging and alarms.

The IOC will house the timing system, fast ADC(s), digital I/O module(s) and will have a Siemens S7 PLCs connected via Ethernet. One of the PLCs will be used for control of all

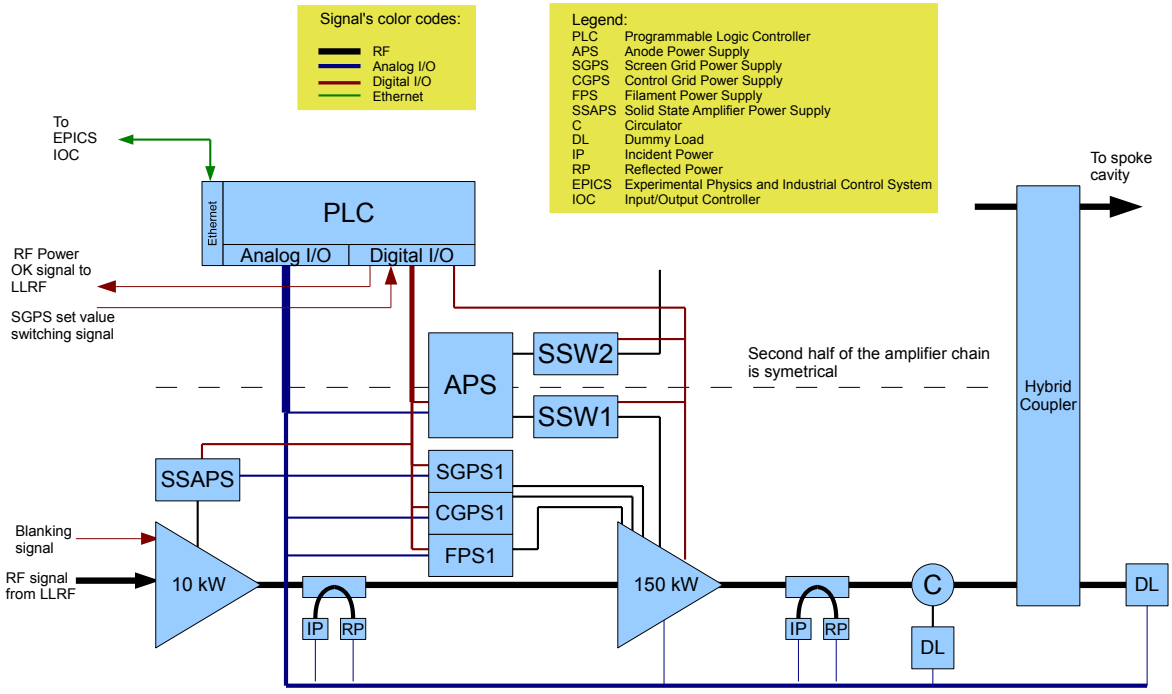

Figure 7: RF power distribution control.

power supplies and amplifiers used in the RF power distribution system for one spoke cavity. The schematic view of the system controlled by this PLC is presented in Fig. 7. Other PLCs will control the cryogenic plant and personnel protection system

The LLRF and timing systems (to be supplied by ESS) will be added to FREIA as soon as they are available (definitely before the tests of the cryomodule). Until then we plan to rely on laboratory equipment (signal generators, oscilloscopes, network analyzers) and COTS RF modules controlled via LabVIEW. There is a solution for integrating the LabVIEW controlled system with EPICS and if it turns out necessary we will do it.

5 Tetrode power supply

To provide the nominal RF power of 300 kW to the ESS spoke cavity the RF power amplifier at the FREIA Facility is designed with two tetrodes of 150 kW power each. An appropriate tetrode for this power level and required frequency is, for example, the water-cooled tetrode TH 595 manufactured by THALES. The proposed amplifier will operate as a grounded grid tube, see Fig. 8 in which a schematic illustration of the tetrode with connected power supplies is shown. For each tetrode four power supplies are required for anode, filament, screen and control grids. The requirements on the power supplies are given in Table 8 [26].

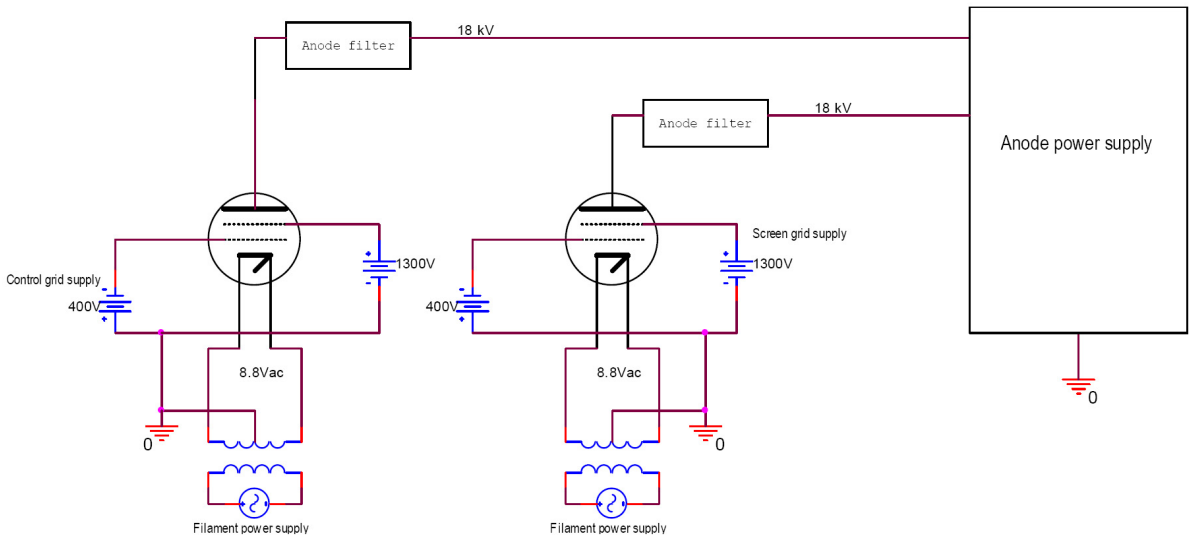

Figure 8: Schematic of DC circuit of tetrodes and the power supplies .

The power supplies for the tetrode are designed in such a way that the amplifier will meet the ESS requirement: running cycle is 14 Hz with 2.86 ms pulses. Other requirements from ESS are high efficiency, water cooling to use the dissipated heat for the district heating in Lund, no oversizing, even loading of the power grid, high reliability and a minimum of maintenance.

5.1 Anode power supply

The most complicated and important of the tetrode power supplies is the anode power supply, which has to deliver most of the power. The maximum pulsed power to the anodes for one amplifier system is 612 kW and the average power is only 25 kW. The output performance of the anode power supply is listed in Table 9.

The tetrode amplifiers are not sensitive to the voltages of the anodes: a change of up to 10 percent will not affect the performance of the amplifiers. This makes it possible to use the same voltage source for both amplifiers. The pulsed mode of operation decides the topology of the anode power supply as it is shown in Fig. 9. Using one common anode power supply will reduce cost and size compared to the use of two power supplies. This is not applicable to the other power supplies because their corresponding voltages have to be

Table 8: *Table of requirements.*

Power supplies	Maximum voltage	Maximum current	Remarks
Anode	18 kV	2 outputs 18 A each	voltage and power regulated
Screen grid	1300 V	700 mA	slew rate better than 0.1 V/μs
Control grid	-400 V	-3 A	2 quadrant operation
Filament	8.8 V AC	190 Arms	voltage ramping

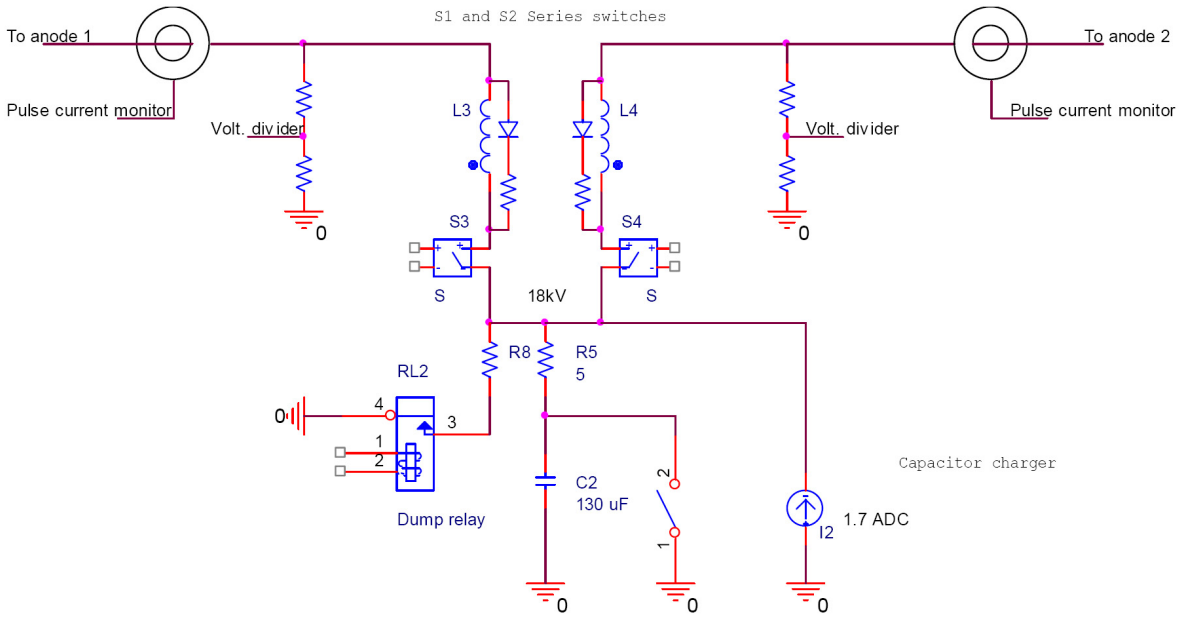

Figure 9: Schematic of the anode power supply.

adjusted individually. If one tetrode fails the anode can be disconnected by its series switch in the anode power supply. See fig. 9.

We can tolerate 10 percent anode voltage droop during the pulse and we may go down to an anode voltage of 16.5 kV. That gives us an admissible total droop of 1 kV. A pulse current of 36 A (18 A per anode) and a ripple of less than 1 kV at 14 Hz will not be a challenge for the capacitor so that a voltage source that can deliver 17 kV and 2*18 A pulses will be a capacitor. This capacitor will be continuously charged by a power source of 25 kW CW. The value of the capacitor is determined by the voltage droop we can tolerate during the RF pulse. There will be a voltage drop over the capacitor series resistor, the series switch and the dI/dt limiting inductor as well.

The voltage drop of the resistor R5 is 180 V at 36 A and the voltage drop of the series switches are approximately 30 V. The inductors will be designed to allow the rise time of the RF-pulse that is 15 μs without limiting the pulse (we require the amplifier rise time to be much smaller than the natural cavity filling time equaling $2Q_L/\omega = 135\mu$s). Let us subtract the voltage drops originating from the resistor and series switch from the 1 kV total voltage drop that we assumed will be allowed and compensate these drops with a bigger capacitor.

Table 9: *Output performance of the anode power supply.*

Output voltage unloaded	18	kV
Output voltage during pulse of 18 A	17	kV
Series switches self-opening	27	A

The voltage droop over the capacitor is reduced to 790 V. The following simple equation

$$Q = C \cdot U = I \cdot t$$

gives C2 = 130 μF for a allowed voltage droop of 790 V.

The resistor R5 must have low resistance to keep the power losses low. The value of the inductance is a tradeoff between low short circuit current and low voltage drop when turning on and off the RF. A compromise for the risetime of the current will be 15 μs for a step from 0 to 18 A. If we set as a limit the same 790 V for an anode current step from 0 to 18 A in 15 μs, then the maximum inductance according to

$$U = L \cdot \frac{dI}{dt}$$

will be approximately 0.7 mH. An air wound coil is suitable. It can be wound with high voltage cable so each turn can withstand the full voltage when there is a short circuit in the load. The short circuit current rate occurring during a pulse will be less than 26 A/μs.

The series switches must open fast at a short circuit in the load to protect themselves from overcurrent and, of course, to protect the amplifier. Switch off time from 60 ns to 3 μs for the switch itself are standard values found in the datasheets. To be conservative we take the 3 μs switch off time and add 3 μs to sense the output short. The worst case to have a short circuit is when the RF pulse is ongoing. The short circuit current from the anode power supply will rise from 18 A to 96 A. The output voltage will be very low and the energy in the short circuit will be low, most of the energy will come from the capacitors of the anode filter. The series switches have the advantage of not discharging the capacitor and the RF-amplifier can be back in operation a few ms after a temporary short circuit or malfunction of the tetrodes. The series switches need to have intrinsic reversed diodes so that the switches can survive reversed voltage. Each output will be equipped with voltage and current monitors. A voltage divider can have a bandwidth of 5 to 10 MHz and a current transformer approximately 10 MHz maximum frequency.

The capacitor charger could be of different topologies. It will charge with 1.7 A up to 18 kV so that the maximum output power will be 31 kW. The charger has to be power and voltage regulated so that by regulating the power the capacitor is charged just to reach the desired voltage. A slow regulation loop can fix this. The loading of the power grid will be constant in spite of the pulsed output current.

A dump relay to discharge the capacitor is needed for personal safety as well as a switch directly connecting the capacitor to ground. Care has to be taken of how the return current flows from the amplifiers.

5.2 Screen grid power supplies

They can be common off the shelf laboratory power supplies. The maximum output of 1300 V and maximum output current of 0.7 A result in 910 W required. The output performance of the screen grid power supplies is listed in Table 10.

To protect the screen grid power supplies from discharges from the anodes a high voltage diode will be connected in series with the output, and a spark gap and a burden resistor in parallel with the output as shown in Fig. 10. The resistance of the bleeder must be so low

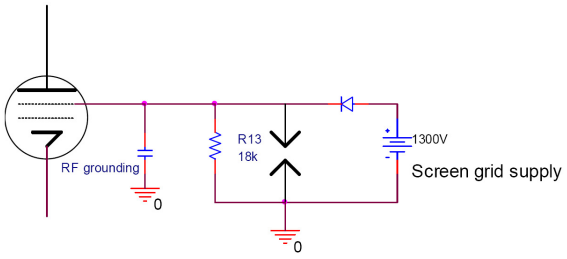

Figure 10: Schematic of the screen grid connection.

that the current exceeds the current flowing to the grid in a static mode. The average screen grid current is 26 mA and the screen grid voltage 900 V. Let the bleeder current be 50 mA. The value of the resistor is then 18 kOhm.

In case of malfunction in the amplifier or short circuit the screen grid power supplies must be first to reduce the voltage by switching off or being set to zero. If the screen grid voltage exceeds the anode voltage, the power dissipated in the screen grid will be too high and an oscillation in the tetrode itself may start. In order to get a quick cut off of the anode current the output capacitance of the screen grid power supplies shall not be greater than the capacitance of the RF-grounding.

5.3 Control grid power supplies

They shall have negative outputs with a voltage of 400 V, other parameters are given in Table 11. The RF input amplitude applied to the cathode is so high that the voltage of the control grid referred to the cathode can be positive and then rectify the RF input signal. It will be good if the control grid power supplies can source and sink the output current.

Such two quadrant laboratory power supplies are available. The outputs will have burden resistors as well. There must be no spark gaps on the output as they would take away any control of the tetrode. In order to regulate the anode current quickly the control grid power supplies will have a short step response from 10 to 90% of output voltage change in less than 7 ms.

Table 10*: Output performance of the screen grid power supplies.*

Output voltage	1300 V
Output current	700 mA
Output power	910 W
Output capacitance	lower than the RF-grounding capacitance

5.4 Filament power supplies:

AC-supplies are preferable because of high current and low voltage on the output. Output voltage is 8.8 Vrms and output current 190 Arms. The output performance of the filament power supplies is given in Table 12. The secondary cables must have a large cross-sectional area to carry 190 Arms. The output transformers can be place closed to the amplifiers and the secondary cables can be short.

A high current low voltage AC power supply cost less than a DC power supply. For example, the output current does not have to be rectified. The regulating component may be a triac in an AC power supply. The output voltage shall be ramped from zero to 8.8 V in 8 minutes by an internal voltage ramp generator. The filament power supplies shall have black heat voltage of 2.5 V when the amplifier is off in order to improve the lifetime of the tetrodes due to thermal cycling.

5.5 Possible technical risks

In the anode power supply the series switches are an issue. The current capability of the switches is not very high, 250 A. Current sense must be fast acting to signal to the series switch to open before the current becomes too high at a short circuit. The $\frac{dI}{dt}$ limiting inductors in series with the switches limit the current at a short circuit. At the same time, these inductors, together with the anode filters, may restrict the fast amplitude response of the amplifiers. The lifetime of the capacitor is also an issue. The circuits of the control grids where the input RF voltage to the cathode is so high that the control grids have a higher potential then the cathode thus rectifying the RF signal.

5.6 The start-up sequence of the power supplies

The startup sequence of the power supplies must be as follows:

1. Filament power supplies ramping up from zero to 8.8 V in 8 minutes;
2. Control grid power supplies on;
3. Anode power supply on;
4. Screen grid power supplies on.

Shut down is done in reversed order. In case of a malfunction in the amplifier the screen grid power supplies must be switched off/set to zero as without screen grid voltage the anode current will be cut off.

Table 11: *Output performance of the control grid power supplies.*

Output voltage	-400 V
Output current	3 A with current sink capability
Step response -150 V to -400 V	in less than 5 ms

Table 12: *Output performance of the filament power supplies.*

Output voltage	8.8 V AC
Output current	190 Arms
Voltage ramping	0 to 8.8 V in 480 s
Black heat voltage	2.5 V AC

6 High-power RF test at the FREIA Facility

6.1 Power supply test

The DC power supplies for TH595 tetrodes will be built by industry according to the FREIA specification described above. Testing of the power supply will be also done in industry with participation of specialist from the FREIA group. The main steps of power supplies testing will be as follows.

Anode power supply:

- Check all actual interlocks.
- Check for water leaks if water cooled.
- Test security system, door opened, emergency stop.
- Check the operation of the dump relay.
- Wire test performed at each output. Start tests with 9 kV anode voltage, if successful increase to 18 kV. The wire shall be 0.2 mm Cu 36 cm long.
- Connect two 1 kΩ 18 kV minimum 25 kW resistors to each output.
- Close and open the output switches one at a time and monitor the output current and voltage at the built in monitors. Record the measured voltage and current on a digital oscilloscope.
- Change to 100 kΩ 18 kV at least 4 kW resistors at the output.
- Check the absolute output voltage with an external voltage divider that has an accuracy better than 1%. Adjust the output voltage if needed.

Filament power supplies:

- Check all actual interlocks.
- Check for water leaks if water cooled.
- Test the eventual security system: door opened, emergency stop.

- Connect a 46.3 mΩ 2 kW resistor to output.
- Ramp up the voltage to 8.8 V during 8 minutes.
- Check the voltage across the resistor with a precision true rms voltmeter better than 1% accuracy.
- Check output current resistor with a precision true rms ampere meter better than 1% accuracy.

Screen grid power supplies:

- Check all actual interlocks.
- Test the external interlock.
- Connect a 1857 Ohm 1 kW resistor to the output.
- Check the absolute output voltage with external voltage divider that has an accuracy better than 1%. Adjust the output voltage if needed.

Control grid power supplies:

- Check all actual interlocks.
- Test external interlock.
- Connect a 133 Ohm 1.2 kW resistor to the output.
- Check the absolute output voltage with external voltage divider that has an accuracy better than 1%. Adjust the output voltage if needed.

6.2 Testing of the high-power amplifier and components

When building an amplifier and components for accelerator applications, one of the factors taken into consideration is the ability to work into a poor match. Situations where amplifiers run into perfect loads with no mismatch are rare. In fact, during the transient regime accelerating cavities are always mismatched to amplifiers. At the same time, because of the reflected power the gain of the RF amplifier operating into the poor match is lower than that of the amplifier operating into a good match [22]. Therefore, the tetrode amplifier at the FREIA test stand is protected by a circulator in order to not only avoid amplifier damage but also to have a high gain. Hence, the circulator is an important part of the amplifier and to test it in the amplifier chain, the amplifier has to be tested not only with a matched load but also with a variable short. During the high-power test we will use the variable short to create adverse conditions for the amplifier and test the RF distribution system under different electric and magnetic fields patterns. The main steps of the testing procedure will be :

- low-power characterization of all components using VNA;
- high-power testing of all components, especially the circulators and measurement of their insertion loss;
- testing of the preamplifiers on a dummy load;
- testing of the high-power amplifiers on a dummy load;
- testing of the high-power amplifiers on a sliding short for different phases of reflection.

Firstly, as we mentioned the S characteristics of all passive components will be measured by using a standard network analyzer. Then, the dependence of the output power and phase on the input power will be measured individually for each amplifier to check for possible discrepancies. When a signal is applied to the input of a device, the output will appear at some later point in time such that the phase delay appears. Phase will be measured and recorded as a function of frequency over a specified range. For most vacuum tube devices, phase and amplitude responses are closely coupled. Any change in amplitude that varies with frequency will produce a corresponding phase shift. Recall that the ability to quickly change the amplifier output power level without phase jump is important to model the beam effect during the high-power test of the spoke cavity Finally, we will measure the power performance characteristics of the whole amplifier. The gain and phase responses as well as the response time determined by the amplifier bandwidth and power supply parameters are of main concern because these characteristics directly affect compensation of the spoke cavity beam loading via the feedback system. The phase dynamics during the transient regime or caused by considerable variation of the input power can be characterized by the group delay that will be measured.

6.3 High-power test of the ESS spoke cavity

The spoke cavity is a superconducting TEM type resonator with large velocity acceptance and high mechanical stiffness. Although the spoke cavity was invented more than twenty yeas ago and numerous studies on it have been performed spoke cavities have never been used in a real operating accelerator [28]. The ESS LINAC is expected to be the first LINAC having a spoke section to accelerate the beam at intermediate beam energies. Therefore, careful testing of the spoke cavity is important for reliable operation of the ESS LINAC. Below we discuss components and features of the spoke cavity that need special care and comprehensive testing. Studies of the spoke cavity to be performed at FREIA Facility:

- reach nominal accelerating gradient
- perform conditioning of the cavity coupler
- measure static and dynamic Lorentz force detuning
- study electroacoustic stability of the cavity
- test the cavity tuner
- implement a reliable and automatized adaptive feed-forward compensation system

6.3.1 Cavity test stand

During design and commission of the high-power FREIA test stand we will use broad experience gained at other laboratories like DESY [29], Fermi [7] and Jefferson [30] Laboratories. Our test stand is expected to consist of four main blocks: power source, measurement network, control system and a cryomodule with a cavity. The block diagram of the test stand is shown in Fig. 11. The control system being responsible for different testing techniques and interlocks is an essential part of the whole system. In fact, a comprehensive study of the cavity requires two different testing regimes: the phase locked loop configuration and fixed RF frequency regime. The former allows to track the cavity frequency. A phase locked loop is a feedback loop designed to keep the phase between the RF source and the cavity voltage at a given constant value. To this end the measured cavity voltage is compared to the set value (maximal achievable voltage for a given RF power source and cavity coupling) and the difference is dynamically sent to a PID controller that generates appropriate correcting signal. This signal being mixed with a signal from the signal generator gives the frequency equal to the current value of the cavity frequency. Thus, the phase between the RF source and the cavity voltage is kept constant. The filling pattern of a cavity is determined by the setting of this phase and is independent of the dynamic variation of the cavity frequency. The fixed RF frequency regime with a special step-wise variation of the power pulse will be used to test the cavity tuning system under conditions similar to those in an accelerator. This testing technique is discussed in detail below.

Unlike a low-power test, there is generally an excessive cost associated with recovery from damaging a cryomodule or failure of a high power coupler. In addition, much higher RF power available is capable of producing prompt damage. For these reasons, full interlocks must be applied to the cryomodule when more than a few Watts of RF are applied to it [30]. The interlocks will include a subset of the following: coupler arc, both air side and vacuum side, infrared detectors for monitoring window temperatures, coupler vacuum, cavity vacuums, helium pressure, helium level and coupler cooling water flow. When a fault

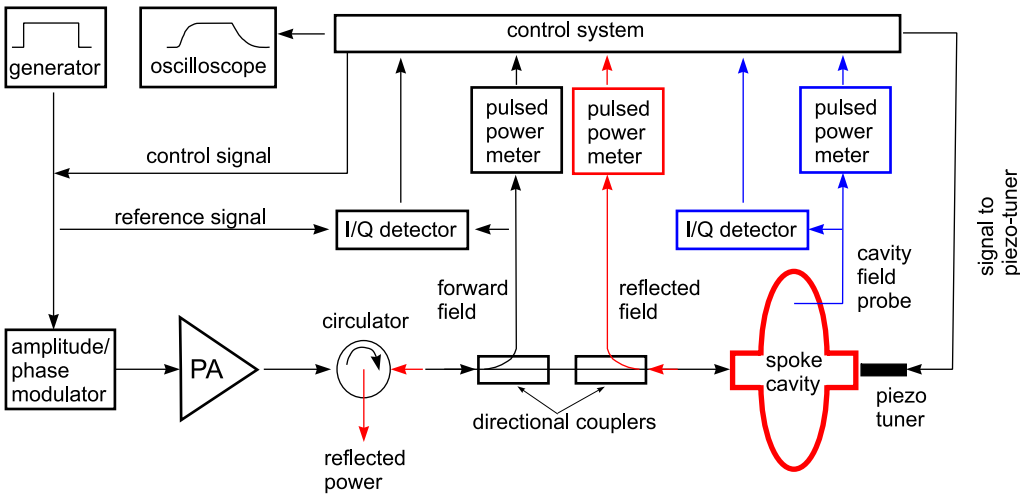

Figure 11: A simplified schematic of the FREIA high-power test stand.

in one of these interlocks occurs the LLRF drive signal will be interrupted using both a PIN switch at the low power part for a fast reduction in applied RF power and an RF relay for a high-voltage isolation. The control system should also switch off the primary power fed to the high voltage power supply in the event of an unsafe condition.

6.3.2 Measurement of the accelerating gradient

The baseline measurement for the gradient at FREIA facility will be an emitted power measurement along with the measurement based on data from the calibrated antenna. The latter will be calibrated during low-power tests at IPN Orsay and the calibration at high-power test will be checked using an emitted power measurement. In fact, a simple decay measurement is unappropriate for over coupled cavities. Specifically, when a cavity is strongly over coupled the reflected power is almost equal to the forward power in the steady-state regime and the error in the lost power, which determines the gradient, is extremely high. For example, a 5-cell CEBAF cavity, which has a frequency of 1.5 GHz and a loaded-Q of $6.6 \cdot 10^6$, the value of the coupling factor is 1500. Performing a simple decay measurement using the same techniques as used for critically coupled cavities would lead to errors in gradient and Q_0 that were on the order of 3000% [30]. In contrast, the emitted power measurement allows one to measure the cavity gradient with an accuracy of 5% to 7% and the Q-external from about 10% to 12% [30].

6.3.3 Study of the Lorentz detuning

As we mentioned, the Lorentz force detuning causes a mismatch between cavity and generator and to keep the voltage ratings constant during the beam pulse, the RF input power amplitude and phase must be adjusted. Compensation of the dynamic detuning effects with the RF system requires providing additional RF power. To avoid wasting RF power the scheme based on a dynamic tuning of the cavity frequency by piezoelectric tuners has been proven to be a viable choice [31]. If the Lorentz detuning is properly canceled by the piezoelectric tuner action, the cavity frequency remains stable during the beam pulse and the cavity operation is optimal. To optimize the frequency compensation scheme by a piezoelectric tuner, a clear understanding, modeling and measurement of the full detuning dynamics is needed. To this end one should perform detailed experimental study of a dynamic detuning created by the Lorentz forces and by the piezoelectric tuner action.

One should distinguish between the static and dynamic Lorentz detuning observed during CW and pulsed tests. In general, increasing the boundary stiffness will decrease the static Lorentz force detuning. Contrary to the static Lorentz force detuning behavior, increasing the boundary stiffness does not necessarily decrease the dynamic Lorentz force detuning [32]. Therefore, dynamic Lorentz force detuning experiments need to be performed. Once the test is made, recommendations to reduce the dynamic Lorentz force detuning can be made.

Measuring of the spoke cavity mechanical parameters and dynamic Lorentz force detuning will be done at FREIA operating the cavity in the self-exciting mode. In this case the cavity voltage amplitude is independent of the detuning and this fact simplifies the extraction of the mechanical parameters associated with the radiation pressure action [33]. The cavity should be excited in CW (a few kW is sufficient) and small modulations of the RF current applied to generate sinusoidal variations of the voltage amplitude which produce in turn sinusoidal

variations of the Lorentz forces. The transfer function linking the RF current modulations to the detuning is obtained by fixing the amplitude of the RF current modulations and by sweeping the frequency of these modulations.

6.3.4 Study of the piezoelectric tuner action

The coupling of the piezoelectric to the cavity is inherently different than the coupling of the Lorentz forces because the action of the piezoelectric tuner is local whereas the action of the radiation pressure is distributed along the structure. For example, the piezoelectric tuner mounted in the SNS medium beta cavities results in coupling to the longitudinal modes but not to the transverse modes [33]. To optimize the piezoelectric input voltage waveform, mechanical parameters of the dressed cavity are needed. To study the piezoelectric tuner action the cavity will be operated under closed feedback loop control of the RF using two different methods adopted from Fermilab experience [7]:

- Drive the piezo tuner with a swept sine wave while exciting the cavity in CW mode (a few kW is sufficient). Changes in the response of the cavity phase will be monitored.
- Measure the voltage induced on the piezo as the cavity is driven by an RF pulse.

Note that similar tests at low power will be performed at IPN Orsay but no power coupler will be mounted into the cavity so that the test of the piezoelectric tuner has to be repeated for the cavity equipped with the coupler. The latter will change normal frequencies of the cavity.

The cavity should be equipped with geophones mounted on the flange at the tuner end in order to directly measure the longitudinal and transverse vibrations of the cavity and the coupling between them. Additional geophones should be mounted on the support structure below the cavity inside the cryostat in order to measure vibrations induced by external sources. To fully characterize the vibrational characteristics of the cavity the following transfer functions have to be measured: cavity detuning response to the piezo, geophone response to the piezo and to the Lorentz Force. Such analysis is needed to study electroacoustic stability of the cavity.

6.3.5 Conditioning the cavity coupler

Conditioning the cavity coupler will be done together with colleagues from IPN Orsay and CEA Saclay using their long-term experience.

6.4 Summary

More than a dozen of spoke resonators prototypes (SSR, DSR, TSR) have been constructed and tested worldwide. None have accelerated beam until now and the ESS LINAC will be the first accelerator to operate with spoke cavities. Experience with other types of superconducting cavities indicates that high-power test is vital for reliable operation of the cavity in an accelerator. Although characteristics of a bare cavity can be obtained in a low-power test some important features of a 'dressed' cavity like the electroacoustic stability and tuning system can be studied only in a high-power test stand. The ESS LINAC is a

pulsed machine and the Lorentz detuning originating from the electromagnetic pressure on the cavity walls is expected to be strong. The Lorentz force along with the cavity sensitivity to mechanical excitations at some resonant frequencies may lead to self-sustained mechanical vibrations which make cavity operation difficult. Practical experience shows that increasing the boundary stiffness will decrease the static Lorentz force detuning but not necessarily the dynamic one. Therefore, the FREIA group at Uppsala University is building a high-power test stand able to study performance of the ESS spoke cavity at high power. The RF test stand will be able to drive the cavity not only in the self-excitation mode but also with closed RF loop and fixed frequency. The later technique will be used to reproduce the shape of the cavity voltage pulse as it is expected to be in the cavity operating in the ESS LINAC such that the cavity tuning compensation system will be tested under realistic conditions.

References

[1] R.A. Yogi et al., 'Selection of RF Power Source and Distribution Scheme at 352 MHz for Spoke Cavities at ESS and FREIA,' Uppsala University, FREIA Report 2012/01 (2012).
http://urn.kb.se/resolve?urn=urn:nbn:se:uu:diva-174458

[2] R. Seviour, 'Comparative Overview of Inductive Output Tubes,' ESS report, June 2012.

[3] S. Pegg, 'Conceptual Design Report,' ESS-2012-001, 2012.

[4] S. Molloy, Linac power optimisation including beam-velocity effects, ESS report: January 25, 2012.

[5] S. Pegg, R. Kreier, 'ESS Technical Design Report,' September 28, 2012.

[6] T.P. Wangler, 'RF linear accelerators,' WILEY VCH, 2008, 450 p.

[7] R. Carcagno, J. Branlard, B. Chase, H. Edwards, D. Orris, Y. Pischalnikov , A. Makulski, J. Reid, W. Schappert, 'First fermilab results of srf cavity lorentz force detuning compensation using a piezo tuner,' Proc. of SRF2007 workshop, TUP57, 2007.

[8] G. Devanz, P. Bosland, M. Desmons, E. Jacques, M. Luong, B. Visentin, 'Compensation of Lorentz force detuning of a ttf 9-cell cavity with a new integrated piezo tuner,' Proc. of EPAC06 conf., pp. 378-380, 2006.

[9] W. Hofle, 'Update on SPL LLRF activities,' 4th SPL/ESS collaboration Meeting, Lund, June 30, 2010.

[10] H. Padamsee, 'RF superconductivity,' WILEY VCH, 2009, 448 p.

[11] V. Goryashko, V. Ziemann, R. Yogi, R. Ruber, 'Amplitude and Phase Control of the Accelerating Field in the ESS Spoke Cavity,' Procc. of LINAC12 conf., TUPB107, 2012.

[12] THALES, 'TH781: high-power tetrode,' technical specification ST2_781. http://www.thalesgroup.com/Portfolio/Security/Tetrodes_for_particle_accelerators

[13] THALES, 'TH391: high-power tetrode,' technical specification 56998694. http://www.thalesgroup.com/Portfolio/Security/Tetrodes_for_particle_accelerators

[14] THALES, 'TH595: high-power tetrode,' technical specification 62396375. http://www.thalesgroup.com/Portfolio/Security/Tetrodes_for_particle_accelerators

[15] Thales, private communication.

[16] Thales, private communication.

[17] 'Care and feeding of power grid tubes,' edited by R.I. Sutherland, EIMAC division of Varian, 1967.

[18] R.G. Carter, 'Review of RF power sources for particle accelerators,' Proc. of CERN accelerator school, p. 269, 1992.

[19] E. Montesinos, 'CERN SPS Upgrade: New 200 MHz and 800 MHz amplifiers,' 15th ESLS-RF Workshop, 5-6 October 2011, Grenoble, France.

[20] J. Walter, 'Techniques to extend the service life of high-power vacuum tubes,' NAB Engineering Conference Proc., Washington DC, 1994.

[21] K. Walter, 'Materials and Technologies for Vacuum Tubes,' Courtesy of Walter Welch, 1960.

[22] J.C. Whitaker, 'Power Vacuum Tubes,' Boca Raton: CRC Press LLC, 2000.

[23] P. Marchand, T. Ruan, F. Ribeiro, and R. Lopes, 'High power 352 MHz solid state amplifiers developed at the Synchrotron SOLEIL,' Phys. Rev, STAB 10, 112001 (2007).

[24] http://www.synchrotron-soleil.fr/portal/page/portal/Instrumentation/AmpliSolide

[25] D. Vandeplassche L. M. Romao, 'MYRRHA Accelerator R&D Program,' SLHiPP-2, LNS-INFN, Catania, Italy, 2012.

[26] R. Wedberg et al., 'Power Supplies for Tetrode High Power Amplifiers at FREIA,' Uppsala University, FREIA Report 2012/02 (2012). http://urn.kb.se/resolve?urn=urn:nbn:se:uu:diva-182119

[27] D. Sun, D. Wildman, R. Madrak and D. Horan, 'Power Test of a 325 MHz Hybrid for Fermilab Proton Driver,' The Fourth CW and High Average Power RF Workshop, Argonne, USA, 2006.

[28] S. Bousson, 'A walk down the Linac,' presented at the 'ESS AD RETREAT', 5th December 2011, Lund.

[29] H. Weise, 'Superconducting rf structures test facilities and results,' Proc. of the 2003PAC Conference, 673, 2003.

[30] T. Powers, 'Practical Aspects of SRF Cavity Testing and Operations,' SRF Workshop 2011, Tutorial Session.

[31] S. Simrock, 'Lorentz Force Compensation of Pulsed SRF Cavities,' Proc. LINAC2002, WE204, 2002.

[32] R. Mitchell, K. Matsumoto, G. Ciovati, K. Davis, K. Macha, R. Sundelin, 'Lorentz force detuning analysis of the spallation neutron source (SNS) accelerating cavities,' Proc. of the 10th Workshop on RF Superconductivity, p. 236, 2001.

[33] M. Doleans, 'Studies in reduced-beta elliptical superconducting cavities,' PhD Thesis, Paris, 2003.